Records of Natural Products

www.acgpubs.org

SHORT REPORT

Penioxalone A: A new isocoumarine derivative from *Penicillium oxalicum* with potent cytotoxic effects on A549 cells

Chiluan Ma[1], Yimeng Li[2], Siyu Liu[2], Jing Ren[2], Jian Wang[3*] and Wenbin Gao[2*]

[1]Department of Thoracic Radiation Oncology, Cangzhou Central Hospital, Cangzhou, 061000, China
[2]College of Life Science, CangZhou Normal University, Cangzhou, 061000, China
[3]College of Chemistry and Chemical Engineering, Cangzhou Normal University, Cangzhou, 061000, China

Abstract: A chemical analysis of *Penicillium oxalicum*, a fungus isolated from saline soil, resulted in the discovery of four bioactive compounds (**1**–**4**), including a new isocoumarine derivative, named penioxalone A (**1**). The structural characterization of penioxalone A was achieved through comprehensive spectroscopic techniques, including 1D and 2D NMR spectroscopy coupled with HRESIMS data. To determine its absolute configuration, experimental data from ECD and ORD were compared with theoretical calculations. The cytotoxicity of compounds **1**, **3**, and **4** was assessed against A549 human lung carcinoma cells, revealing IC_{50} values of 3.6, 0.23, and 0.35 μM, respectively. These compounds exhibited enhanced potency compared to cisplatin, a standard chemotherapy drug, which had an IC_{50} of 4.2 μM.

Keywords: Fungus, *Penicillium oxalicum*, penioxalone A, resorcylic acid lactone, cytotoxic activity

Cite this article as:
Ma et al. Penioxalone A: A new isocoumarine derivative from *Penicillium oxalicum* with potent cytotoxic effects on A549 cells. (2026). *Records of Natural Products*, 20(2):e25113716

Received: *02 November 2025*
Revised: *27 December 2025*
Accepted: *01 January 2026*
Published: *12 January 2025*

1 Fungal Source

In August 2022, a fungal strain identified as *Penicillium oxalicum* GWB07-3 was obtained from soil from a saline environment in Huanghua, Hebei Province, China. The strain was characterized by means of molecular identification using the internal transcribed spacer (ITS) region of rDNA, and the resulting sequence was uploaded to GenBank under the accession number PX473044. This strain is currently maintained at the College of Life Sciences, Cangzhou Normal University.

2 Previous Studies

Saline soil-derived fungi are increasingly recognized as an important source of bioactive natural products, owing to their adaptation to harsh environmental conditions (Zhang et al., 2023; Planes & Caballero-George, 2015). Species of the *Penicillium* genus—a dominant genus in these environments, are particularly noted for producing a variety of bioactive compounds, including resorcylic acid lactones, which exhibit significant antimicrobial, anticancer, and cytotoxic activities (Liu et al., 2024; Sritharan et al., 2024). Specifically, *Penicillium oxalicum* has gained attention due to its capacity to produce novel bioactive metabolites (Wang et al., 2022; Zhang et al., 2022). For example, a recently identified resorcylic acid lactone from *P. oxalicum* showed potent cytotoxicity against human liver cancer cells (HepG2), with an IC_{50} value of 0.32 μM (Gao et al., 2025). These findings highlight *P. oxalicum* as a promising source of cytotoxic agents for cancer treatment.

3 Present Study

In this study, a new isocoumarine derivative, penioxalone A (**1**), was isolated from saline soil-derived *P. oxalicum* GWB07-3, along with three previously identified compounds: dihydroresorcylide (**2**) (Zhang et al., 2015), penicillixanthone A (**3**) (Tan et al., 2019), and secalonic acid D (**4**) (Ren et al., 2006) (Figure 1). This work provides a detailed isolation, structural elucidation, and biological assessment of these compounds.

The strain *P. oxalicum* GWB07-3 was cultured in 500 mL flasks, each containing 60 g of rice and 60 mL of distilled H_2O, and incubated for 30 days at 28°C. After fermentation, the mycelial mass was subjected to successive extractions with dichloromethane (CH_2Cl_2) and methanol (MeOH) in a 1:1 ratio until the extract was clear. The resulting crude extract (62 g) was concentrated under reduced pressure. Liquid-liquid extraction was performed six times with ethyl acetate (EtOAc) and water, until the EtOAc phase was colorless. The concentrated EtOAc extract (35 g) was subjected to vacuum liquid chromatography (VLC) using a gradient of petroleum ether (PE) and EtOAc, producing five fractions (Fr.1–Fr.5). Fraction Fr.2 was further purified using silica gel

*Corresponding Authors: Jian Wang. Email: wangjian3790@126.com; Wenbin Gao. Email: wenbinxing@caztc.edu.cn

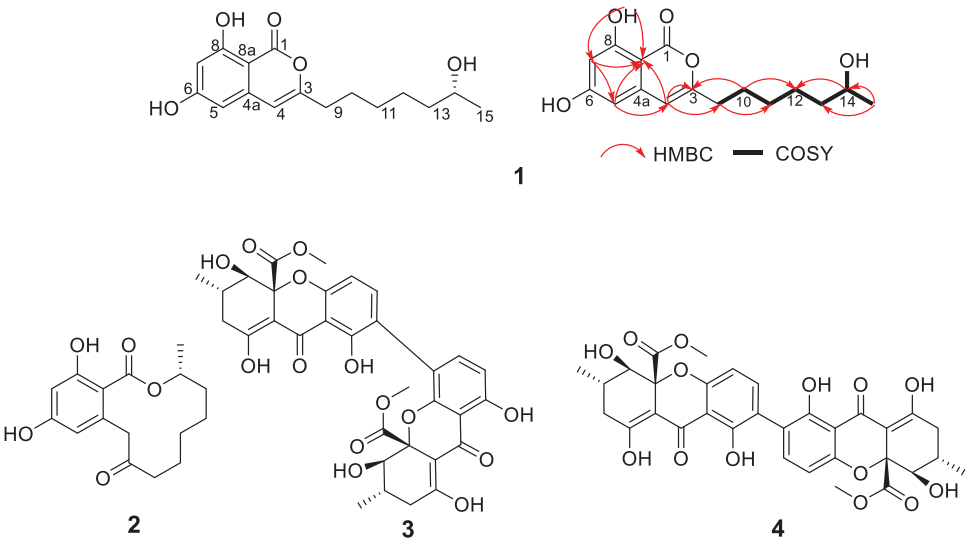

Figure 1. Chemical structures of **1**–**4**, along with the Key 2D NMR correlations for **1**, illustrating the molecular framework of **1**

chromatography (80:20 PE/EtOAc), yielding two subfractions, Fr.2.1 and Fr.2.2. Compound **1** (10.9 mg) was isolated from Fr.2.1 by Sephadex LH-20 gel chromatography (PE: CH_2Cl_2:MeOH, 2:1:1) and semi-preparative HPLC. Compound **2** (23.3 mg) was isolated from Fr.2.2 using silica gel chromatography (CH_2Cl_2:MeOH, 20:1). For Fr.4, Sephadex LH-20 gel chromatography (CH_2Cl_2:MeOH, 1:1) was first employed to remove contaminants, followed by further purification with silica gel chromatography (CH_2Cl_2:MeOH, 20:1), resulting in compounds **3** (5.5 mg) and **4** (5.2 mg).

Penioxalone A (***1***)*:* White solid; $[\alpha]_D^{20}$ = 6.8 (*c* = 0.08, MeOH); UV (MeOH) λmax (log ε) 234 (4.2), 257 (3.9), 328 (3.5) nM; ECD (*c* 0.10 mM, MeOH) λmax ($\Delta\varepsilon$) 203 (0.2), 236 (–1.3), 247 (1.6) nM; HREIMS: *m/z* 291.1240 (calcd. 291.1238 for $C_{16}H_{19}O_5^-$). ^{1}H (600 MHz) and ^{13}C (150 MHz) NMR data (see Table 1).

ECD and ORD calculations: The 3D chemical structures of the two enantiomers of **1**, (14*R*)-**1** and (14*S*)-**1**, were constructed, and their lowest-energy conformations within an energy window of 10.0 kcal/mol were obtained using Spartan software with the MMFF94 force field. For (14*R*)-**1** and (14*S*)-**1**, 432 and 438 conformations were obtained, respectively, and these conformations were optimized at the B3LYP/6-31G(d) level using Gaussian 09 (Frisch et al., 2009) for the first round. Then, a second round of optimization was carried out, selecting the conformations with energy differences of less than 2.5 kcal/mol, for further refinement with the B3LYP/6-311+G(d) basis set. The ECD and ORD data for these conformations were calculated using Gaussian 09 at the B3LYP/6-311+G(d,p) level. Finally, using SpecDis 1.64 software (Bruhn et al., 2013), Boltzmann statistics were applied to simulate the spectra based on the relative energies of the conformations, and the resulting spectra were compared with the experimental results.

Bioactive Assay: The cytotoxic effects of compounds **1**–**4** were evaluated against A549 human lung carcinoma cells using the MTT assay (Ciapetti et al., 1993). Cisplatin was selected as a positive control in this study. The IC_{50} values were derived from the dose-response curves obtained through nonlinear regression analysis. All experiments were conducted in triplicate.

Compound **1** was isolated as a white solid and identified through its HRESIMS and NMR data. The HRESIMS spectrum displayed a deprotonated molecular ion at *m/z* 291.1240 ($[M-H]^-$), consistent with the molecular formula $C_{16}H_{20}O_5$, indicating seven degrees of unsaturation. The NMR spectra (^{1}H, ^{13}C, and HSQC) revealed a substituted aromatic ring with two meta-coupled protons at δ_H 6.35 and 6.30 (*J* = 2.4 Hz), alongside carbon signals at δ_C 139.7, 102.6, 165.5, 101.4, 162.7, and 98.1. A carbon signal at δ_C 165.7 indicated the presence of a lactone, while the singlet at δ_H 6.48 and the associated carbon signals at δ_C 157.4 and 103.8 suggested a trisubstituted olefin, confirming a resorcylic acid lactone framework (Bang & Shim, 2020). A detailed comparison of the NMR data revealed that compound **1** was structurally similar to the known compound stutter α-pyrone (Xu et al., 2014). The main difference between the two compounds lay in the C-9 and C-10 positions. In stutter α-pyrone, the signals for the disubstituted double bond between C-9 and C-10 (δ_C 122.8, CH and 137.1, CH; δ_H 6.11, 1H, d, *J* = 15.4 Hz and 6.60, 1H, m) were replaced in compound **1** by two secondary carbon signals (δ_C 32.3, CH_2 and 26.3, CH_2; δ_H 2.46, 2H, dd, *J* = 7.2, 7.8 Hz and 1.59, 2H, m). This suggested that the C-9 to C-10 double bond in stutter α-pyrone was reduced to a saturated bond in compound **1**. This hypothesis was supported by the key HMBC correlation signals in **1** from H-4 to C-9, H-9 to C-11, and H-10 to C-3 and C-12 (Figure 1). These data confirmed the isocoumarine derivative core and established the planar structure of compound **1**.

Compound **1**'s absolute configuration was deduced through computational and experimental optical analysis. Specifically, its electronic circular dichroism (ECD) spectrum aligned closely with the simulated spectrum of the (14*R*) enantiomer, with consistent Cotton effect

http://doi.org/10.25135/rnp.2511.3716
Rec. Nat. Prod. 2026, 20(2):e25113716

Table 1. NMR data for compound **1** in DMSO-d_6 and the known stutter α-pyrone in pyridine-d_5

Pos.	1		Stutter α-pyrone [a]	
	δ_H (J in Hz)	δ_C	δ_H (J in Hz)	δ_C
1		165.7, C		166.4, C
3		157.4, C		152.7, C
4	6.48, s	103.8, CH	6.36, s	103.2, CH
4a		139.7, C		140.8, C
5	6.35, d (2.4)	102.6, CH	6.70, s	104.7, CH
6		165.5, C		167.8, C
7	6.30, d (2.4)	101.4, CH	6.83, s	105.6, CH
8		162.7, C		164.8, C
8a		98.1, C		99.8, C
9	2.46, dd (7.2, 7.8)	32.3, CH_2	6.11, d (15.4)	122.8, CH
10	1.59, m	26.3, CH_2	6.60, m	137.1, CH
11	1.30, m	28.5, CH_2	2.23, m	33.3, CH_2
12	1.36, m	25.0, CH_2	1.77, m	25.9, CH_2
	1.29, m		1.69, m	
13	1.30, m	38.9, CH_2	1.67, m	39.9, CH_2
			1.56, m	
14	3.55, m	65.7, CH	4.02, m	67.1, CH
15	1.02, d (6.6)	23.7, CH_3	1.35, d (6.6)	24.7, CH_3
8-OH	10.96, s			
14-OH	4.30, s			

Note: [a]NMR data from the previous report (Xu et al., 2014).

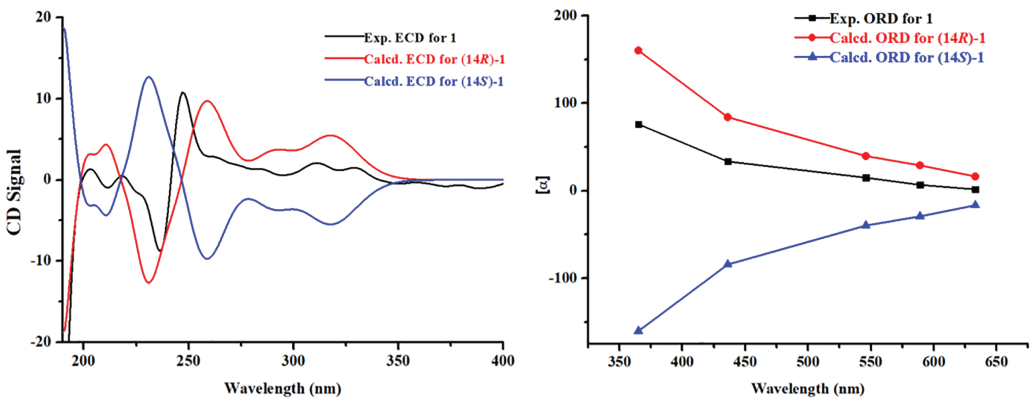

Figure 2. The ECD and ORD spectra for **1**, including experimental and computed data

patterns observed between 200 and 350 nM (Figure 2). In addition, the ORD profile of **1** was in good agreement with the computed data for (14*R*)-**1** within the 350–650 nM wavelength range, further confirming the assignment. Collectively, these ECD and ORD results conclusively determined the absolute configuration of **1** as 14*R*.

In determining the absolute configuration of **1**, it initially seemed that the C-14 chiral center, being distant from the chromophore, would have little impact on the ECD and ORD spectra based solely on the planar structure. However, to clarify why computed ECD and ORD were still used to confirm the absolute configuration, it is necessary to consider the 3D conformation of the molecule. Upon closer examination, it was found that, in solution, the molecule did not adopt an extended chain conformation. Instead, the C-14 hydroxyl group twisted to form a medium-strength hydrogen bond with the ester carbonyl group at C-1. This interaction forced the molecule into a more rigid 6/6/12 tricyclic structure (**1a**), which was energetically more stable than the extended form (**1b**), with an energy difference (ΔE = 2.2 kcal/mol), as shown in Figure 3. This conformational rigidity brought the C-14 chiral center much closer to the chromophore, making it possible to determine the absolute configuration of **1** using the computed ECD and ORD spectra.

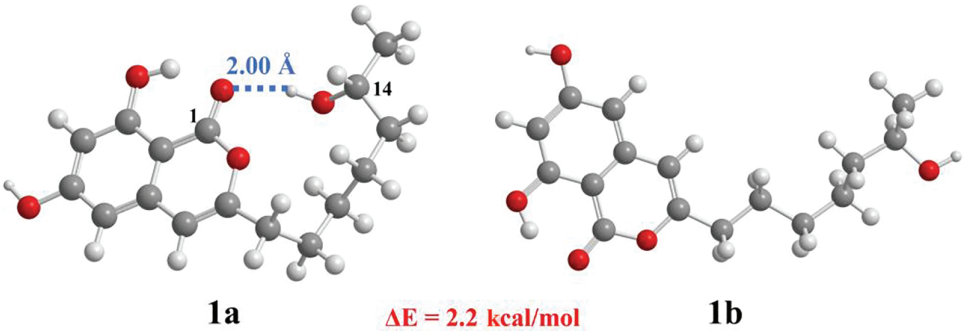

Figure 3. The 3D structures of two possible conformations (**1a** and **1b**) for **1**

Based on the structural similarity of compound **3** to previously reported compounds with antitumor activity (Xu et al., 2023), we conducted cytotoxicity testing to evaluate its potential anticancer properties. We evaluated the cytotoxic effects of compounds **1**–**4** against A549 cells. Among them, compound **3** exhibited the strongest activity, with an IC_{50} value of 0.23 μM, followed by compound **4** (IC_{50} = 0.35 μM) and compound **1** (IC_{50} = 3.6 μM). All three compounds showed greater potency than the positive drug cisplatin (IC_{50} = 4.2 μM) under the same assay conditions. These findings suggested that the resorcylic acid lactone scaffold contributed significantly to the observed cytotoxicity, and that subtle structural differences, such as hydroxylation at C-14 in **1**, may influence the activity profile. The notably strong potency of compound **3** warrants further investigation as a potential anticancer lead.

Funding Statement

This work was financially supported by the Self-funded Project of the Cangzhou City Key Research and Development Program (No. 213106050).

Author Contributions

Chiluan Ma: Funding and Writing original manuscript; Yimeng Li: Methodology and Formal analysis; Siyu Liu: Visualization and Investigation; Jing Ren: Validation and Data curation; Jian Wang: Writing-review & editing and Project administration; Wenbin Gao: Methodology, Writing-review & editing and Project administration.

Availability of Data and Materials

The authors declare that the data supporting the findings of this study are available within the paper and its Supplementary Information files. Should any raw data files be needed in another format they are available from the corresponding author upon reasonable request. Source data are provided with this paper

Ethics Approval

This study involved only in vitro biochemical assays and the use of isolated compounds. No human articipants or live animals were involved.

Conflicts of Interest

The authors declare that they have no competing financial interests.

Supporting Information

Supporting Information accompanies this paper on http://www.acgpubs.org/journal/records-of-natural-products.

ORCID

Chiluan Ma: 0000-0002-1803-3156
Yimeng Li: 0009-0004-8926-7883
Siyu Liu: 0009-0007-9177-013X
Jing Ren: 0009-0005-0523-6914
Jian Wang: 0009-0005-9524-8387
Wenbin Gao: 0009-0001-8178-2520

References

Bang, S. & Shim, S. H. (2020). Beta resorcylic acid lactones (RALs) from fungi: Chemistry, biology, and biosynthesis. *Archives of Pharmacal Research*, *43*, 1093–1113. DOI: 10.1007/s12272-020-01275-6.

Bruhn, T., Schaumlöffel, A. N. U., Hemberger, Y. & Bringmann, G. (2013). SpecDis: Quantifying the comparison of calculated and experimental electronic circular dichroism spectra. *Chirality*, *25*, 243–249. DOI: 10.1002/chir.22138.

Ciapetti, G., Cenni, E., Pratelli, L. & Pizzoferrato, A. (1993). *In vitro* evaluation of cell/biomaterial interaction by MTT assay. *Biomaterials*, *14*, 359–364. DOI: 10.1016/0142-9612(93)90055-7.

Frisch, M. J., Trucks, G. W., Schlegel, H. B., Scuseria, G. E., Robb, M. A., Cheeseman, J. R., Scalmani, G., Barone, V., Mennucci, B., Petersson, G. A., Nakatsuji, H., Caricato, M., Li, X., Hratchian, H. P., Izmaylov, A. F., Bloino, J., Zheng, G., Sonnenberg, J. L., Hada,

M., Ehara, M. et al. (2009). *Gaussian 09*. Wallingford, CT, USA: Gaussian Inc.

Gao, Y., Li, W. & Ruan, H. (2025). The chemical and biological properties of natural resorcylic acid lactones. *Natural Product Reports*, *42*, 1387–1410. DOI: 10.1039/d5np00033e.

Liu, D., Ma, L., Rong, X., Kang, H. & Liu, W. (2024). Spirolones A–E, five spiroketals from a productive saline soil derived *Penicillium raistrickii*. *Frontiers in Microbiology*, *15*, 1495396. DOI: 10.3389/fmicb.2024.1495396.

Planes, N. & Caballero-George, C. (2015). Marine and soil derived natural products: A new source of novel cardiovascular protective agents targeting the endothelin system. *Planta Medica*, *81*, 630–636. DOI: 10.1055/s-0034-1396205.

Ren, H., Tian, L., Gu, Q. & Zhu, W. (2006). Secalonic acid D; A cytotoxic constituent from marine lichen-derived fungus *Glio-cladium* sp. T31. *Archives of Pharmacal Research*, *29*, 59–63. DOI: 10.1007/bf02977469.

Sritharan, T., Salim, A. A., Khalil, Z. G. & Capon, R. J. (2024). Jugiones A–D: Antibacterial xanthone-anthraquinone heterodimers from Australian soil-derived *Penicillium shearii* CMB-STF067. *Antibiotics*, *13*, 97. DOI: 10.3390/antibiotics13010097.

Tan, S., Yang, B., Liu, J., Xun, T., Liu, Y. & Zhou, X. (2019). Penicillixanthone A, a marine-derived dual-coreceptor antagonist as anti-HIV-1 agent. *Natural Product Research*, *33*, 1467–1471. DOI: 10.1080/14786419.2017.1416376.

Wang, Y., Chen, W., Xu, Z., Bai, Q., Zhou, X., Zheng, C., Bai, M. & Chen, G. (2022). Biological secondary metabolites from the *Lumnitzera littorea*-derived fungus *Penicillium oxalicum* HLLG-13. *Marine Drugs*, *21*, 22. DOI: 10.3390/md21010022.

Xu, H., Shen, X., Li, X., Yang, X., Chen, C. & Luo, D. (2023). Dehydrocurvularin (DSE2), a fungal-derived macrolide, induces apoptosis of gastric cancer cells by activating PARP-1 and caspase-3. *Apoptosis*, *28*, 525–538. DOI: 10.1007/s10495-023-01811-x.

Xu, Y., Zhou, T., Zhang, S., Espinosa-Artiles, P., Wang, L., Zhang, W., Lin, M., Gunatilaka, A. A. L., Zhan, J. & Molnár, I. (2014). Diversity-oriented combinatorial biosynthesis of benzenediol lactone scaffolds by subunit shuffling of fungal polyketide synthases. *Proceedings of the National Academy of Sciences*, *111*, 12354–12359. DOI: 10.1073/pnas.1406999111.

Zhang, D., Li, S., Fan, M. & Zhao, C. (2023). The novel compounds with biological activity derived from soil fungi in the past decade. *Drug Design, Development and Therapy*, *16*, 3493–3555. DOI: 10.2147/dddt.s377921.

Zhang, Y. H., Li, L., Li, Y. Q., Luo, J. H., Li, W., Li, L. F., Zheng, C. J. & Cao, F. (2022). Oxalierpenes A and B, unusual indole-diterpenoid derivatives with antiviral activity from a marine-derived strain of the fungus *Penicillium oxalicum*. *Journal of Natural Products*, *85*, 1880–1885. DOI: 10.1021/acs.jnatprod.2c00322.

Zhang, P., Meng, L. H., Mándi, A., Li, X. M., Kurtán, T. & Wang, B. G. (2015). Structure, absolute configuration, and conformational study of resorcylic acid derivatives and related congeners from the fungus *Penicillium brocae*. *RSC Advances*, *5*, 39870–39877. DOI: 10.1039/c5ra02203g.